JOURNAL OF CATALYSIS **179,** 503–514 (1998)
ARTICLE NO. CA982245

Heat of Adsorption of Carbon Monoxide on a $Pt/Rh/CeO_2/Al_2O_3$ Three-Way Catalyst Using *in-Situ* Infrared Spectroscopy at High Temperatures

Tarik Chafik,[1] Olivier Dulaurent, Jean Louis Gass, and Daniel Bianchi[2]

*Laboratoire d'Application de la Chimie à l'Environnement (LACE), UMR 5634, Université Claude Bernard, Lyon-I, Bat. 308 43 Bd du 11 Novembre 1918, 69622 Villeurbanne, France

Received March 24, 1998; revised August 5, 1998; accepted August 6, 1998

The adsorption of CO (1% CO/He mixture) on a 2.9% Pt/0.6% Rh/20% CeO_2/Al_2O_3 (in weight percent) three-way catalyst is studied in the temperature range 300 K–800 K by FTIR spectroscopy using a suitably infrared cell of small volume. The quantitative treatment of the spectra leads to the determination of the evolution of the coverage of the adsorbed species with the temperature. The main adsorbed species is the linear CO form characterized by an IR band at 2063 cm^{-1}, probably formed on platinum atoms. The heat of adsorption of this species is determined at various coverages in the range $0.36 < \theta < 1$. In agreement with the literature, a linear relationship is observed between the heats of adsorption and the coverage. The values determined at each coverage (i.e. 116 kJ/mol at $\theta = 0.8$ and 148 kJ/mol at $\theta = 0.36$) are similar to those obtained from calorimetric measurements on platinum-supported catalysts. Similar results are obtained on two platinum-containing solids: 2.9% Pt/Al_2O_3 and 2.4% $Pt/20\%$ CeO_2/Al_2O_3. The procedure described to determine the heat of adsorption of adsorbed CO species at various coverages using FTIR spectroscopy is experimentally easy. However, the disproportionation reaction, $2\,CO \rightarrow C_{ads} + CO_2$ which may arise at high temperature, limits its application to a specific range of temperatures.

I. INTRODUCTION

The *in-situ* characterization of the surface state of a catalyst during a reaction is one of the major objectives in heterogeneous catalysis. Transient experiments have been proven to be powerful tools in this field, in particular for the reactions involving carbon monoxide (with H_2, O_2, NO) on metal supported catalysts ((1–7) and references therein). They involve the creation of a controlled perturbation of the gas/surface state obtained in dynamic (flow) conditions and the measurement of responses of the gas-phase compositions. The perturbation is either physical (i.e. increase of the temperature) or chemical (i.e. change of the composition of the gas phase). Generally the experiments are performed at atmospheric pressure and the change of the gas-phase composition is followed by using a mass spectrometer as a detector. The fast response of this technique, as well as a properly designed reactor and sampling system, give quantitative data on the number and the reactivity of the adsorbed species. However, a lack of information on the chemical structure of the adsorbed species exists and other detectors such as the FTIR spectrometer become important. A suitably designed IR cell permits us to study the effects of the perturbations on the adsorbed species (8–10). In particular, the volume of the cell must be small (i.e. 1–2 cm^3 or less) in order to perform transient experiments under conditions close to those used with a classical differential reactor. The first part of the present paper describes an IR cell capable of performing transient experiments (small dead volume), in the temperature range 300–900 K, with CaF_2 windows which allow us to study the infrared bands of adsorbed species in the IR range 4000–1050 cm^{-1}. In a second part, this cell is used to determine the heat of adsorption of CO-adsorbed species on a three-way catalyst $Pt/Rh/CeO_2/Al_2O_3$ related to the change of the coverages with the temperatures of adsorption. Monometallic solids Rh/Al_2O_3, Pt/Al_2O_3, and $Pt/CeO_2/Al_2O_3$ are also studied and the results are compared to those observed on the three-way catalyst.

The determination of the heats of adsorption of CO on unsupported platinum (film, foil, and single crystal) have been obtained using various experimental methods referenced by Vannice *et al.* (11). The values are in the range 80 kJ/mol–180 kJ/mol (11). Some difficulties arise to determine the heat of adsorption of gases (i.e. CO) on metal-supported catalysts. For instance, TPD methods which may lead to the activation energy of desorption of adsorbed CO species, usually equal to the heat of adsorption, taking into account that the adsorption of CO is not activated, are influenced by various parameters as the diffusion, the readsorption, and the reactor design (12–14). Nowadays, the values

[1] Present address: Faculté des Sciences et Techniques de Tanger, Université Adbelmalek Essadi, B.P 416-Tanger-Maroc, Morocco.

[2] To whom correspondence should be addressed.

0021-9517/98 $25.00

of the heat of adsorption of gases as CO and H_2 on supported platinum catalysts are obtained using microcalorimetric measurements (15–17). The values determined are similar to those found on unsupported platinum and reveal the change of the heat of adsorption with the coverage (16), as is found on various single crystals. In the present study, we use the change of the intensity of the FTIR spectra of adsorbed CO species with the temperature of adsorption (range 300–800 K), to determine the heat of adsorption of CO on a $Pt/Rh/CeO_2/Al_2O_3$ three-way catalyst and on two platinum containing solids: Pt/Al_2O_3 and $Pt/CeO_2/Al_2O_3$.

II. EXPERIMENTAL

(a) Catalysts

The 2.9% Pt/0.6% Rh/20% CeO_2/Al_2O_3 (in wt%) catalyst is prepared via co-impregnation of a 20% CeO_2/Al_2O_3 powder prepared initially by the incipient wetness method. Alumina (Degussa C γ-Al_2O_3, BET area 100 m^2/g) is impregnated with aqueous solution of $Ce(NO_3)_3$, 6 H_2O (Aldrich), using the incipient wetness method. After drying 12 h at room temperature and then 24 h at 373 K, the solid is treated at 877 K in air during 2 h (heating rate 5 K/min). The noble metals are impregnated on the 20% CeO_2/Al_2O_3 powder using an appropriate amount of aqueous solution of H_2PtCl_6, xH_2O and $RhCl_6$, $3H_2O$ (Aldrich). After drying 12 h at room temperature and then 24 h at 373 K, the solid is calcined in air at 673 K, leading to a surface area of 70 m^2/g. The noble metal content is obtained using the *inductively coupled plasma* method after acidic dissolution of the catalyst powder. The ratio Pt/Rh = 4.8 has been selected because it corresponds to the one used on commercial three-way catalysts. For the FTIR study, the catalyst is compressed into a disk ($\Phi = 1.8$ cm, weight = 70 mg) which is placed in the sample holder of the IR cell described below. For determination of the efficiency of the solid as a three-way catalyst, it is deposited on a cylindrical monolith structure ($\Phi = 2.5$ cm, L = 5.5 cm) to obtain a precious metal loading of 15 g/ft^3, similar to the values used in commercial monoliths for a vehicle. Three others catalysts have been prepared following the same method of preparation: 0.5% Rh/Al_2O_3, 2.9% Pt/Al_2O_3, 2.4% Pt/20% CeO_2/Al_2O_3.

Before the adsorption of CO, the solids are treated *in situ* (150 cm^3/min), according to the following procedure: oxygen ($T = 713$ K, $t = 30$ min) → helium ($T = 713$ K, $t = 30$ min) → hydrogen ($T = 713$ K, $t = 1$ h) → helium ($T = 713$ K, $t = 10$ min) → helium (adsorption temperature).

(b) Catalyst Characterization

The dispersion is obtained from the adsorbed quantities (μmol/g of catalyst) of gas (CO and H_2), measured with a quadrupole mass spectrometer as the detector, according to a procedure previously described (18). In particular, the system allows us to study the modifications of the composition of a gas mixture at the outlet of a quartz reactor during a switch between two controlled flows of gas under atmospheric pressure, i.e. He → 5% CO/5% Ar/He.

(c) Efficiency of the $Pt/Rh/CeO_2/Al_2O_3$ Solid as a Three-Way Catalyst

The performances of the solid as a three-way catalyst are determined by an analytical system previously described (19–20). Mainly, synthetic gas mixtures (CO/NO/propene/propane/O_2/CO_2/H_2O/N_2) of compositions similar to automobile exhaust gas are used to determine with an hourly space velocity similar to real conditions (75000–100000 h^{-1}) the efficiency of catalysts deposited in monolith structures ($\Phi = 2.5$ cm, L = 5.5 cm). The performances are characterized by studying the conversion of the pollutants as a function either of the inlet gas temperature (light-off) or of λ, the air–fuel equivalence ratio (without and with perturbation of the value of λ). The composition of the gas at the outlet of the stainless steel reactor which gives the conversions of the reactive gas is determined by FTIR spectrometry.

(d) High Temperatures IR Cell for Transient Experiments

The IR cells built in the past and used for catalytic studies were designed to realize the *in-situ* treatment of the catalyst in a controlled atmosphere and at temperatures (450–1100 K) high enough to activate the catalyst (21–22). Some models of IR cells allow to use high pressures (>1 atm) and low temperatures (liquid nitrogen). The design of the cell must also meet some practical requirements such as a convenient way to change the catalyst, the cost of the cell, and its maintenance. The main technological difficulties encountered in achieving the requirements come from the IR window. First, materials with good IR transmission (NaCl, KBr, and CaF_2) have generally limited mechanical properties and are very sensitive to thermal shocks. Second, the windows must be sealed to the body of the cell mainly made of glass, quartz, or stainless steel. The common materials used for this sealing (23) have poor or limited thermal stability (epoxy cement, Viton, or Kalrez O-ring). Another problem arises from the introduction of the catalyst (generally compressed into a pellet) in the cell. This requires some mobile parts with the use of an O-ring gasket (Viton, copper, or gold) or an equivalent system which is also temperature sensitive.

For classical applications, two types of IR cells (A and B) have been developed (transmission mode) to take into account the above difficulties mentioned (21–22). The IR cells of model A are designed to separate the thermal treatment of the catalyst from the IR beam path. This approach keeps the sensitive part of the cell at low temperature. After the treatment, at high temperature (1100 K and above using quartz material) the catalyst is moved in the beam path with

an appropriate system for subsequent analysis (24–25). The IR cells of model B allow the treatment of the catalyst directly in the IR beam path (26–30). The problems related to the IR windows can be solved by (a) increasing the distance between the heater and the windows, (b) using a material of low thermal conductivity (Pyrex or quartz), and (c) working at low pressure. The volume of the cell can be reduced (around 100 cm^3) and a conducting material can be used with a cooling water jacket associated with the support of the CaF_2 disks. However, for smaller volume the cooling creates a heat loss which limits the maximum temperature obtained and also creates conditions where thermal shocks may appear. Hydride cells have been used to combine the advantages of the two types of cells (31).

The IR cells used for transient experiments are of the B type but with a very small volume (1–2 cm^3) in order to perform rapid changes of the gas phase. A small volume also permits an increase in the ratio of the incoming signal due to the adsorbed species with respect to the incoming signal due to the gas-phase species. This may eliminate the contribution of the gas phase to the recorded spectra, in particular during a catalytic reaction. New materials have been used to accommodate the small volume of the cell with basic IR window properties. The ultimate objective is to have the smallest volume and the highest temperature. Penninger was one of the first to propose a solution to the above problems (32). Two CaF_2 disks were sealed into the stainless steel body of the cell by a seal placed around the disk and constituted of alternating soft and hard rings. By compression, the soft parts flow into the hard part and create the desired seal. The catalyst disk was introduced between the two windows with a spacing of 1–3 mm. A temperature of 720 K is reported using Rulon 25 rings as the soft material but the seal was fragile and constituted the weak point of the cell (32). An alternative solution has been proposed by Hicks *et al.* (10). Two CaF_2 windows were sealed on two flanges with Kalrez O-rings and separated by the sample holder. This brought into a volume of 0.4 cm^3, a distance of 2.4 mm between the CaF_2 disks and an upper temperature limit of 590 K. This limit was increased to 673 K using sapphire windows (33). This material has better mechanical properties than CaF_2, but presents an IR transmission cutoff at around 1600 cm^{-1}. This cell is nowadays used (34). Based on this design, various IR-cells/reactors have been constructed. Robbins (35) used either sapphire or CaF_2 windows sealed on metallic flanges and gave a comparative test report. Sapphire appears to be the most reliable solution. For CaF_2 windows, fractures caused by thermal shocks were reported for a heating rate higher than 3.5 K/min and the flange sealing developed leaks under prolonged treatment at 620 K (35). Zhou and Gulari (36) modified a flow-through liquid cell to be used as a transient IR cell. The distance between the two windows was 0.6 mm and the maximum temperature reported was 490 K. Nagai *et al.* (9) have designed an IR cell of 2.5 cm^3 where the flow of gas is forced directly through the disk of the catalyst, limiting the leakage around the edges of the sample. Another high pressure IR cell (37–38) with an upper temperature limit of 530 K, used CaF_2 windows with a path length for the IR beam of 2 mm and a volume 0.2 cm^3.

The upper temperature limit of the above IR cells is the weak point in order to extend applications of the transient experiments to catalytic systems where a high temperature ($T > 700$ K) is required for long periods, either for the activation of the catalyst or for the catalytic reaction. To increase this limit, Chuang *et al.* (39) describe an IR cell of the B type (see above) with a distance between the two CaF_2 windows of 85 mm needed to maintain at 773 K the central part of the cell (where the catalyst is placed) with the temperature of the CaF_2 disks below 523 K (using a cooling water jacket). To obtain the small dead volume necessary to perform transient experiments, two CaF_2 rods, polished on both ends and with dimensions slightly smaller than the body of the cell, are placed between the catalyst pellet and the two CaF_2 windows. The cell permits us to work at high pressure and elevated temperatures (upper limit 873 K). The only problem noted (39), is the care needed during the assemblage of the IR cell/reactor to prevent the cracking of the CaF_2 windows.

In the present work, an IR cell able to attain a temperature of more than 900 K with a distance of 2.2 mm between the CaF_2 windows is described. Two main remarks have been considered for the design of this cell. First, the CaF_2 windows are sensitive to thermal shocks but can hold temperatures as high as 1100 K without modifying their optical and mechanical properties. Second, when a CaF_2 disk ($\Phi = 20$ mm) is placed, without a seal, on a polished metallic flange, the leaks can be as small as 20 cm^3/min for a pressure difference of 1 atm. Figure 1 gives the design of this cell using practical considerations acquired from previous studies (31, 40). More details on the design and performances of the IR cell may be found in (41). This IR cell (stainless steel) have two mobile parts, the sampler holder and the body of the cell (rectangular shape). Two CaF_2 windows ($\Phi = 20$ mm, thickness = 2 mm) can be successively introduced inside the body of the cell through the rectangular hole also used to introduce the sample (Fig. 1, part A). These windows are placed onto a carefully polished flat flange of 2-mm thickness. This gives a 2.2-mm distance between the two windows. Outside the body of the cell, two larger CaF_2 windows ($\Phi = 35$ mm, thickness = 4 mm) are sealed with a Viton O-ring and cooled with a water jacket. The volume between the small and the large windows is continuously evacuated using a mechanical pump (pressure ≈ 1 Pa). The small inside windows are maintained in place by the pressure difference between their two sides. The vacuum in the space between the small and the large windows limits the heat transfer to the outside windows. The gas flow

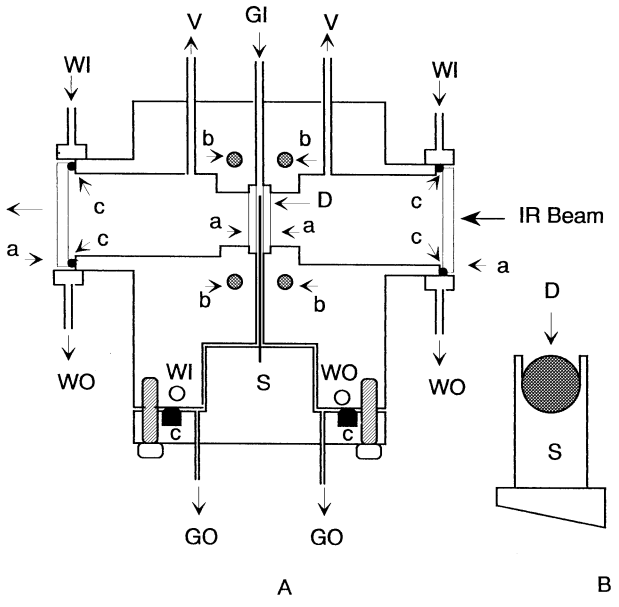

FIG. 1. Design of the high temperature IR cell for transient experiments. (A) Body of the cell; (a) CaF_2 windows; (b) cartridge heaters; (c) Viton O-rings; (V) vacuum line; (GI) and (GO) inlets and outlets of the gases; (WI) and (WO) inlets and outlets of the cooling water jackets; (S) sample holder. (B) Sample holder: (D) disk of catalyst.

(100–2000 cm^3/min) coming from a gas control system for transient experiments (18) is introduced by using a 1/8″ tubing on the top of the IR cell. Another 1/8″ tubing is used for the introduction of a coaxial thermocouple (K type, $\Phi =$ 0.5 mm) placed close to the catalyst pellet. Two outlets of the gases are placed at the bottom of the body of the cell to limit the dead space. Ten 200-W cartridge heaters ($\Phi = 6.5$ mm, $L = 40$ mm) are inserted in the body of the cell (two per hole "b," Fig. 1, and two in vertical holes not shown) and connected to a temperature controller. The maximum heating rate obtained is 15 K/min. The rectangular sample holder ($h = 39$ mm, $l = 24$ mm, thickness $= 1.9$ mm) is made by an assemblage of two plates, leaving an appropriate space for the catalyst pellet ($\Phi = 18$ mm, 30–300 mg) as shown in Fig. 1, part B. The sample holder is fixed on the diameter of a cylinder ($\Phi = 31$ mm, $h = 31$ mm). The hole in the body of the cell where the sample holder is inserted has dimensions 0.2 mm larger than the sample holder. The seal between the body and the sample holder is a Viton graphited O-ring cooled with a water jacket. The cell is placed in an insulated box filled with quartz wool and positioned in the beam of an FTIR spectrometer (either Nicolet 5DX-C or Nicolet Protege).

The seal between the outside windows and the body of the cell has been tested by monitoring its ability to maintain a good static vacuum without having the inside CaF_2 windows and all the inlets and outlets closed. The leaks between the inside CaF_2 windows and the stainless steel body are measured at the outlet of the mechanical pump (atmospheric pressure) with the cell at ambient temperature. Using nitrogen gas (300 cm^3/min at the inlet of the cell) the leaks are of 45 cm^3/min. This value, independent of the flow rate used, decreases with increasing temperatures. The possibility that some gas coming from the mechanical pump could contaminate the catalyst by either effusion or diffusion through the leaks has been studied. After the reduction of the $Pt/Rh/CeO_2/Al_2O_3$ catalyst at 713 K in a hydrogen flow the solid is cooled down to 373 K in helium. The same IR spectra are recorded after the adsorption of CO (see below) whatever the time on stream in helium (range 0–1 h) at 373 K before the switch between He and a 1% CO/He mixture (no oxygen contamination). However, in a vacuum, water is one of the main residual gases and the leaks have been examined with this compound. A pellet (70 mg) of ZrO_2 aerogel is treated at 723 K for 2 h in He followed by 2 h in O_2 (150 cm^3/min) and cooled in helium to room temperature. We have recorded no increase in the intensity of the IR bands of the OH groups at 3770 cm^{-1} and 3680 cm^{-1} (41) during 3 h room temperature. After 6 h at 873 K in helium, the intensities of the IR bands of the OH groups on ZrO_2 decrease by a factor of 5 compared to the signal recorded at 723 K. The upper limit of the IR cell is 923 K. At this temperature, after 2 h, using an O_2 flow, the leaks of the inside windows sharply increase due to a deterioration of the surface of the metallic flanges which need to be polished. For transient experiments, it is necessary to have a fast response of the cell to a controlled change of the gas phase. We have observed (1 scan/s) the increase of the intensity of the CO_2 IR band (2450–2280 cm^{-1}) during a switch from 100 cm^3/min of He to 100 cm^3/min of a 5% CO_2/He mixture. A delay of 10 s is needed to obtain a steady-state concentration of the CO_2 gas. This value, which decreases for higher flow rates, permits us to observe fast changes of the adsorbed species during a transient experiment.

The drawback of the cell is associated with the mechanical pump. If this pump shuts off when the cell is at high temperature, the increase of the pressure into the space between the inside and the outside CaF_2 windows creates a thermal shock leading to the fracture of the outside windows.

III. RESULTS AND DISCUSSION

The present study is focused on the three-way catalyst; however, after the presentation of the FTIR results on this solid, those observed with the monometallic catalysts (Rh/Al_2O_3, Pt/Al_2O_3, and $Pt/CeO_2/Al_2O_3$) are described and compared to the bimetallic catalyst.

(a) Characterization of the Bimetallic Solid

The dispersion of the 2.9% Pt/0.6% Rh/20% CeO_2/ Al_2O_3 (wt%) catalyst is determined using CO and H_2 chemisorption at room temperature. After reduction in H_2 at 713 K,

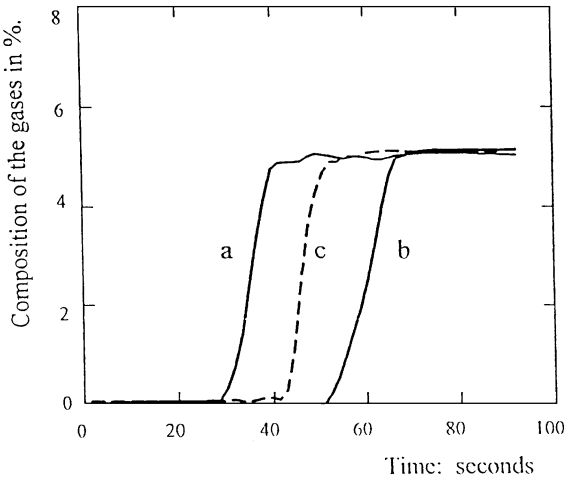

FIG. 2. Adsorption of CO and H_2 at room temperature on the Pt/Rh/CeO_2/Al_2O_3 solid: (a) Argon, (b) CO, and (c) H_2.

the catalyst is cooled down to room temperature in flowing helium (60 cm^3/min). A switch is performed from helium to a 5% CO/5% Ar/He mixture. Figure 2 gives the evolution of the composition of the gases argon (curve a) and CO (curve b) during the switch. The time lag between the two curves indicates the adsorption of CO on the solid. The amount of CO chemisorbed is 75 μmol/g of catalyst. No reversible adsorption of CO is detected during the switch from the CO/Ar/He mixture to pure He. As shown below by FTIR, the adsorption of CO on the Pt/Rh/CeO_2/Al_2O_3 catalyst is mainly a linear adsorbed species on the noble metal part of the catalyst without adsorption onto the CeO_2/Al_2O_3 support. This permits us to consider a chemisorption ratio CO/M = 1 which leads to a dispersion of D = 35%.

A similar experiment is performed but using a 5% H_2/5% Ar/He mixture. Curve c, Fig. 2, gives the evolution of the hydrogen concentration. The difference with the argon signal gives an amount of chemisorbed hydrogen of 32 μmol H_2/g without measurable reversible chemisorption (the minimum amount determined for the reversible chemisorption is 3 μmolH_2/g). Assuming a dissociative adsorption of hydrogen (ratio H/M = 1), the dispersion is D = 31%, in agreement with the value obtained using CO chemisorption. The value of the dispersion agrees with the literature data on Pt/Rh catalysts of similar metal loading: D = 25% on a 3% Pt/1% Rh/Al_2O_3 catalyst (42) and 44% on a 0.5% Pt/0.5% Rh/Al_2O_3 (43–44).

(b) Efficiency of the Pt/Rh Containing Solid as Three-Way Catalyst

For a monolith impregnated with the catalyst, Fig. 3 gives the conversions of CO, NO, and of the hydrocarbons (hydrocarbons mean conversion of both propene and propane) at 723 K, as a function of λ, the air/fuel equivalence ratio. As expected (45–46) for a three-way catalyst, the prepared solid Pt/Rh/CeO_2/Al_2O_3 permits a high conversion for the three pollutants at $\lambda = 1$. The conversion of NO decreases at $\lambda > 1$ (excess of O_2) and the CO conversion decreases at $\lambda < 1$. These curves are similar to those obtained with commercial monolith catalysts (19, 20) with a metal loading of 30 g/ft^3 and a weight ratio Pt/Rh = 5. This result confirms that the lab-prepared catalyst is representative of a commercial three-way catalyst.

(c) FTIR Spectra of CO Adsorbed at High Temperatures on Pt/Rh/CeO_2/Al_2O_3

The *in-situ* IR cell described in the experimental section is used to study the adsorption equilibrium of CO at high temperatures on the reduced three-way catalyst: 2.9% Pt/0.6% Rh/20% CeO_2/Al_2O_3. The pellet of catalyst is reduced in pure H_2 as described in the experimental section and cooled in He down to 363 K. A 1% CO/He mixture (100 cm^3/min) is introduced leading to the appearance of a high intensity IR band at 2063 cm^{-1} associated to a small IR band at 1884 cm^{-1} (spectrum a, Fig. 4). The IR bands are observed at the same position at room temperature. When the temperature is increased between 363 K and 463 K, the intensity of the IR band initially at 2063 cm^{-1} remains constant but a shift is recorded to 2054 cm^{-1} at 463 K (spectrum b, Fig. 4). For higher temperatures, between 463 K and 800 K, the intensity of the IR band progressively decreases as shown in Fig. 5 and the main IR band shifts to lower wavenumbers (2025 cm^{-1} at 800 K), according to a linear relationship (Fig. 6). The first comment on the observed spectra is the absence of adsorbed gem-dicarbonyl CO species on rhodium atoms, as they are usually characterized by two IR bands of similar intensities at 2090 ± 10 and 2030 ± 10 cm^{-1}, as observed on a Pt/Rh/Al_2O_3 catalyst (47) (see also below the results on the monometallic solids). This suggested that

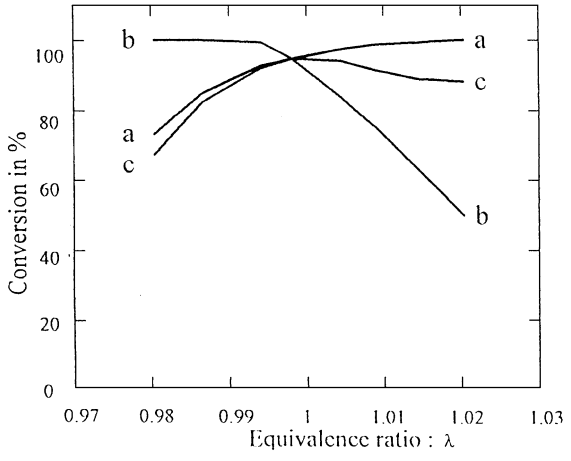

FIG. 3. Efficiency of the Pt/Rh/CeO_2/Al_2O_3 three-way catalyst: conversion of CO (a), NO (b), and the hydrocarbons (c) as a function of λ, the air/fuel equivalence ratio.

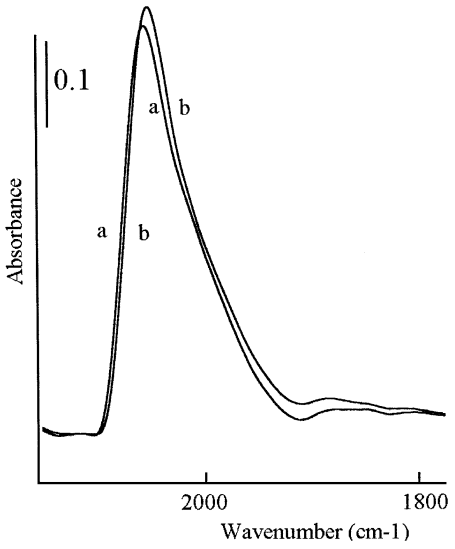

FIG. 4. Infrared spectra taken during the adsorption of CO (1% CO/He) on the $Pt/Rh/CeO_2/Al_2O_3$ three-way catalyst: (a) adsorption at 363 K; (b) adsorption at 463 K.

the rhodium is present in Pt/Rh alloy particles and not as isolated atoms. This conclusion has been proposed by others (48) after adsorption of CO at various temperatures on a 5% weight $Pt/Rh/SiO_2$ catalyst (atomic ratio $Pt/Rh = 1$). The authors (48) observe, on the reduced catalyst, spectra similar to those shown in Figs. 4 and 5, with a high IR intensity band at 2070 cm^{-1} associated with a weak IR band at

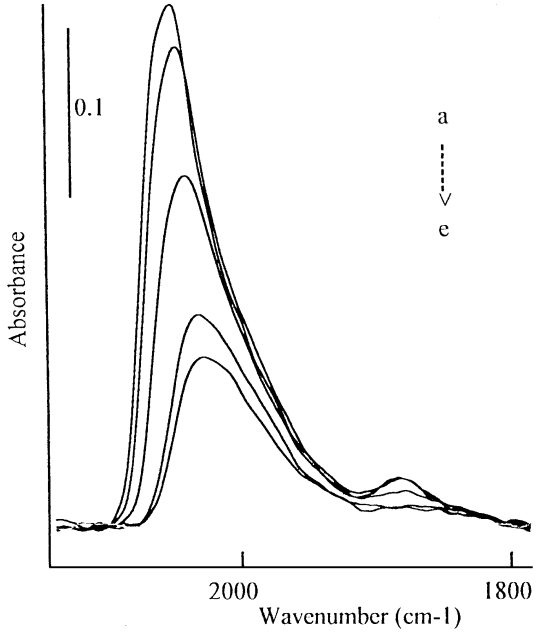

FIG. 5. Infrared spectra taken during the adsorption of CO (1% CO/He) on the $Pt/Rh/CeO_2/Al_2O_3$ three-way catalyst at various temperatures: (a) 440 K; (b) 508 K; (c) 621 K; (d) 713 K; (e) 800 K.

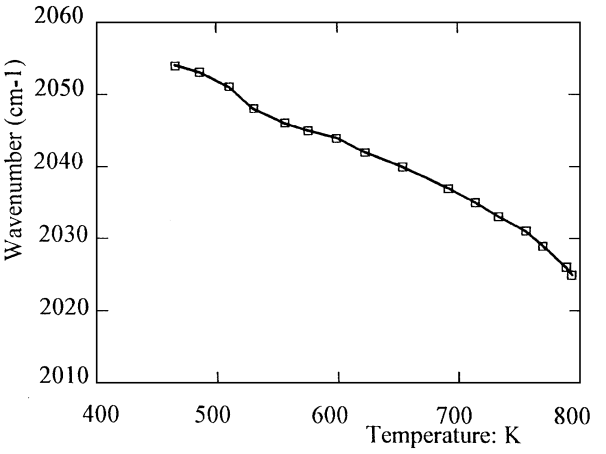

FIG. 6. Shift of the linear CO species with the temperature of adsorption on the $Pt/Rh/CeO_2/Al_2O_3$ solid.

1875 cm^{-1}. The fact that rhodium is not present as isolated atoms is in agreement with various works (42–44) which indicate the presence of bimetallic particles detected after a coimpregnation of Pt and Rh on Al_2O_3, followed by a reduction at high temperature ($T > 573$ K). The surface composition of these particles seems enriched in Pt (42). According to the literature, the adsorption of CO on Pt impregnated on various supports; Al_2O_3 (30, 49, 50, 51), SiO_2 (30, 48, 52), and $CeOx/Al_2O_3$ (7), gives at room temperature a high IR band intensity at 2070 ± 10 cm^{-1} usually associated with a small IR band at around 1850 ± 10 cm^{-1} ascribed to linear and bridged CO species, respectively. On supported Rh catalysts, the linear and bridged CO species give, on various supports MgO (53), SiO_2 (48, 54, 55), Al_2O_3 (56), IR bands at 2070 ± 5 cm^{-1} and 1910 ± 10 cm^{-1} or 1850 cm^{-1} (57), respectively. The above values show that the recorded spectra (Figs. 4 and 5) do not allow us to ascribe, with accuracy, the adsorption sites of CO to either Pt or Rh. However, taking into account that the surface of the Pt-Rh particles can be enriched in Pt (42), we attribute the IR band to linear CO adsorbed on the Pt atoms of the bimetallic particles. This conclusion was also proposed by Van Slooten and Nieuwenhuys on a $Pt/Rh/Al_2O_3$ (48) using different arguments. For the same reasons that above the IR band at 1884 cm^{-1} (Figs. 3 and 5) of the bridged CO species cannot be clearly ascribed to a particular type of sites. However, an IR band observed at 1875 cm^{-1} on a $Pt/Rh/Al_2O_3$ catalyst was attributed to Pt-Rh sites (48) by comparing the shifts of this band observed on Pt and Rh alone and on Pt-Rh alloy.

Remarks. (a) Similar studies of the evolution of the IR band of the linear CO species with the temperature are reported, on a $Pt/Rh/SiO_2$ catalyst (temperature range 300–625 K, CO pressure 2 mbar) (48) and on a 1% Pt/Al_2O_3 catalyst (temperature range 303–573 K, CO pressure 16 mbar) (58) but without a quantitative treatment as described here.

(b) The present observations on the $Pt/Rh/CeO_2/Al_2O_3$ during the adsorption of CO at high temperatures are in agreement with a study on a $Pt/Rh/SiO_2$ catalyst (48) but are different than those observed on a $Pt/Rh/Al_2O_3$ catalyst (47, 58). In this latter study the main adsorbed species at temperature lower than 373 K are gem-dicarbonyl species on the rhodium atoms. However, it must be noted that the treatment of the catalyst with a small partial pressure of CO at $T > 540$ K (47, 58) leads to IR spectra similar to those observed on the present catalyst, with only the IR band of the linear CO at 2044 cm^{-1}.

(d) Heat of Adsorption of CO Linearly Adsorbed on $Pt/Rh/CeO_2/Al_2O_3$

To determine the coverage of the surface with temperatures, it is assumed that the integrated absorption intensity of the linear CO species is constant with (a) the temperature and (b) the coverage as studied by Rasband and Hecker (59) on various Rh/SiO_2 catalysts. Taking into account that the intensity of the IR band is constant between 373 K and 473 K (Fig. 4), it can be concluded that in this range of temperatures, the coverage of the sites is constant and equal to 1. Therefore, the shift of the position of the IR band, in this range of temperatures (Fig. 4) can be attributed to the increase of the temperature because the coverage is constant. The ratio of the surface area of the IR band at a given temperature to the surface area of the IR band at 473 K gives the coverage of the sites at each temperature as shown in Fig. 7. This profile can be compared to the one expected from Langmuir's model for an adsorption without dissociation and given by

$$\theta = LP/(1 + LP) \qquad [1]$$

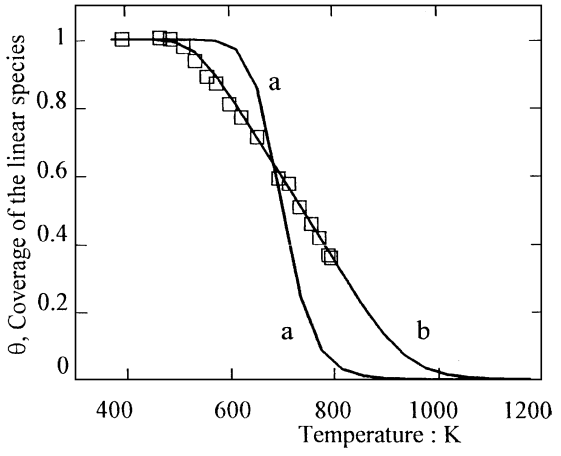

FIG. 7. Evolution of the coverage of the linear CO species with the temperature of adsorption on the $Pt/Rh/CeO_2/Al_2O_3$ solid: □, experimental data; (a) coverage from the Langmuir's model with Ed − Ea = 130 kJ/mol; (b) coverage according to expression [3] (see the text for the parameters).

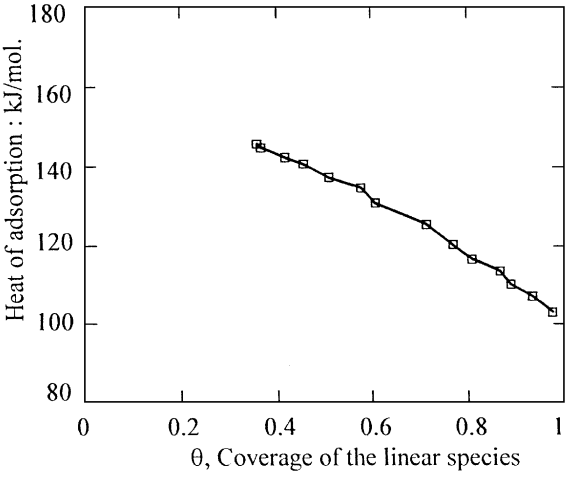

FIG. 8. Change of the heat of adsorption of the linear CO species with the coverage on the $Pt/Rh/CeO_2/Al_2O_3$ three-way catalyst.

with P the pressure of adsorption and L the adsorption coefficient given by the statistical thermodynamic assuming the loss of three degrees of translation:

$$L = \frac{h^3}{k * (2 * \pi * m * k)^{3/2}} * \frac{1}{T^{5/2}} * \exp\left(\frac{Ed - Ea}{R * T}\right) \qquad [2]$$

with h Planck's constant, k Bolztmann's constant, m the weight of the molecule (28×10^{-3} kg/6.02×10^{23}), T adsorption temperature, Ed and Ea the activation energy of desorption and adsorption, respectively, while $Ed - Ea$ is the heat of adsorption. Curve a, Fig. 7, gives the theoretical change of the coverage according to expression [1] and assuming a heat of adsorption of 130 kJ/mol in expression [2]. The difference between the experimental data and the model is due to the fact that the heat of adsorption changes with the coverage of the surface as observed by various studies ((16) and references therein).

Using the experimental data of Fig. 7, the heat of adsorption of CO can be determined for each value of the coverage using expression [1] and considering that the heat of adsorption changes at each coverage. The values are reported on Fig. 8 which shows a linear relationship in the range $\theta = 1$ to $\theta = 0.36$, the lower value of θ obtained at 800 K (see below the explanation of this temperature limit). The values of the heat of adsorption are in agreement with those found on polycrystals and micro crystals of platinum using various analytical methods ((11) and references therein) and on supported platinum catalysts using microcalorimetric methods (11, 15–17). In particular, Sharma *et al.* (16) have obtained on two Pt/SiO_2 catalysts (with two metal dispersions) a linear relationship between $\theta = 0.8$ and $\theta = 0$ from an initial heat of adsorption of 140 kJ/mol to 100 kJ/mol. These values are in agreement with those obtained in the present study: i.e. 116 kJ/mol at $\theta = 0.8$ (Fig. 8). The main

differences between the present results and the study of Sharma *et al.* (16) come from the values between $\theta = 0.8$ and $\theta = 1$. On Pt/SiO_2 (16) the values sharply decrease between 100 kJ/mol to 40 kJ/mol, whereas in Fig. 8 we observe the same decreasing profile in the coverage range 1 to 0.36.

The linear decreasing profile of the heat of adsorption of the linear CO species as observed in Fig. 8 is a classical modification of Langmuir's model leading to the Temkin's model (60, 61). Assuming a linear relationship $E = E_0(1 - \alpha\theta)$, the coverage θ of the sites is given by

$$\theta = \frac{RT}{\Delta E} * \mathrm{Ln}\left(\frac{1 + L_0 * P}{1 + L_1 * P}\right). \qquad [3]$$

where, ΔE is the difference of the heats of adsorption at $\theta = 0$ (E_0) and $\theta = 1$ (E_1), L_0 and L_1 are the adsorption coefficients at $\theta = 0$ and $\theta = 1$ according to expression [2]. Expression [3] leads to Temkin's model assuming $(L_0P) \gg 1$ and $(L_1P) \ll 1$.

Expression [3] permits us to determine the coverage of the linear CO species as a function of the temperature, using $E_1 = 97$ kJ/mol and $E_0 = 178$ kJ/mol to obtain a best fit of the experimental data (values in agreement with Fig. 8). In Fig. 7, curve b, a good agreement can be observed between the model and the experimental observations. The value $E_0 = 178$ kJ/mol is slightly higher than the one measured by Sharma *et al.* (16) on a Pt/SiO_2 and may indicate some interaction of the sites with the various components of the catalyst (bimetallic particles, presence of ceria). On alkali-promoted Pt/SiO_2 catalyst, an increase of the heat of adsorption is observed which leads to values close to 160 kJ/mol at $\theta = 0$ (16). Note also that values of 180 kJ/mol are reported in the literature on unsupported platinum ((11) and references therein).

The upper temperature limit of adsorption studied is 800 K, leading to the lower coverage of 0.36. This is due to the fact that the dissociation of CO according to the disproportionation reaction seems to develop at this temperature and leads to a deposition of carbon on the catalyst and to CO_2 formation. However, this process is very limited with our conditions as shown in Fig. 9 which compares the adsorption of CO before the heating in CO/He to 800 K (spectrum a) and after cooling from 800 K to 463 K in CO/He (spectrum b). A slight decrease of the IR band of the linear CO species is observed without modification of its position. The main differences come from the appearance of the IR bands at 1587, 1518, and 1384 cm^{-1} attributed to the formation of carbonate adsorbed species on the CeO_2/Al_2O_3 part of the catalyst (probably due to the production of CO_2).

Remarks. (a) The adsorption model assuming localized adsorbed species (loss of three degrees of translation) fits very well the experimental data. The increase of the adsorption temperature must lead to the mobility of the adsorbed species which explains, in particular, the rapid attainment of the adsorption equilibrium. However, this mobility does not impose changing the adsorption model, assuming for instance that the adsorbed CO species form a two-dimensional ideal gas. The main argument against this model is that it is observed, with increasing temperatures, a progressive shift of the position of the IR band of the linear species (considered as immobile at room temperature) while its profile is not strongly modified. The mobility of the adsorbed species is not incompatible with the model of localized species (61). Considering the difference between the activation energy of diffusion E_m and the activation energy of desorption E_D: $E_m = (E_D/n)$ with n between 5 and 7 (61) it can be considered that the lifetime of the adsorbed species at a site is longer than its time in flight so that the layer still comprises a localized array (61).

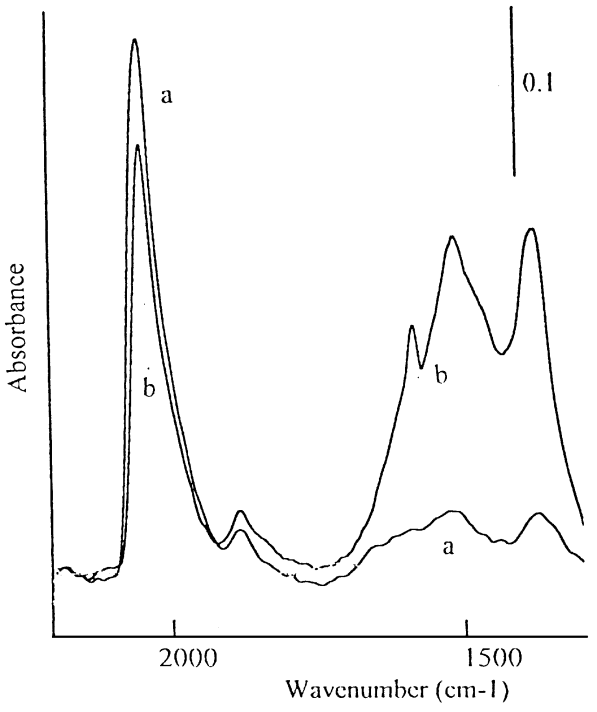

FIG. 9. Infrared spectra taken during the adsorption of CO on $Pt/Rh/CeO_2/Al_2O_3$: (a) at 463 K before the heating at 800 K; (b) after cooling from 800 K to 463 K.

(b) The accuracy on θ is estimated as ± 0.02. This leads to an accuracy, on the values of the heat of adsorption, using expression [1], of ± 2 kJ/mol (for values of θ not too close to 1). However, using expression [3] to fit the experimental profile of θ, the accuracy on E_0 and E_1 is around ± 5 kJ/mol. The above values show that the experimental procedure described is very accurate and can be used to study the influence of various parameters on the heat of adsorption of CO (method of preparation of the catalyst, dispersion, etc.).

(e) FTIR Spectra of CO Adsorbed on the Monometallic Solids

On the reduced 0.5% Rh/Al_2O_3 catalyst, the adsorption of CO (1% CO/He) at 373 K leads to the detection of two IR bands of same intensity at 2092 cm^{-1} and 2020 cm^{-1} attributed to gem-dicarbonyl species. This result was previously observed on reduced 1 wt% Rh/Al_2O_3 catalysts ((58, 62) and references therein). This confirms that the rhodium part of the three-way catalyst is not present as isolated particles because gem-dicarbonyl species are not detected on Figs. 4, 5, and 9. As the adsorption of CO on the Rh/Al_2O_3 catalyst leads to a FTIR spectrum very different from the one observed on the (Pt/Rh)-containing solid, we do not describe in the present study, the evolution of the FTIR spectra on Rh/Al_2O_3 with the adsorption temperature.

On the reduced 2.9% Pt/Al_2O_3 catalyst, the results observed during the heating in 1% CO/He present some differences with those observed on the bimetallic catalyst as shown in Fig. 10. The adsorption of CO at 378 K leads to a spectrum with an IR band at 2073 cm^{-1} (spectrum a) which is attributed to a linear CO species on a reduced platinum atom (30, 49–51) and a very weak IR band at 1850 cm^{-1} (not shown) due to bridged CO species. The increase of the adsorption temperature (Fig. 10, spectrum b) leads to the increase of the intensity of the IR band for temperatures lower than around 480 K associated to a shift to 2067 cm^{-1} at 453 K. For higher temperatures the recorded spectra lead to the following observations: (a) a shoulder is well detected at 2080 cm^{-1} for an adsorption temperature higher than 533 K (Fig. 10, spectrum c); (b) the two IR bands shift to lower wavenumbers (i.e., 2051 cm^{-1} and 2063 cm^{-1} at 783 K for the main IR band and the shoulder, respectively); (c) the surface area of the IR band (the shoulder and the main IR band are not differentiated) is constant between 480 K and 600 K; and (d) the surface area of the IR band decreases for temperatures higher than 600 K (Fig. 10, spectra c–f). Similar results (not shown) are recorded on the 2.4% $Pt/CeO_2/Al_2O_3$: (a) the IR band of the linear CO species on Pt atoms is detected at 2078 cm^{-1} at 373 K in agreement with the position 2070 cm^{-1} observed on a $Pt/CeO_x/Al_2O_3$ catalyst (7); (b) the IR band shifts and its intensity increases between 373 K and 483 K (2063 cm^{-1} at 483 K); (c) a shoulder is well recorded at 2080 cm^{-1} for an adsorption temperature of 530 K; and (d) for temperatures higher than 600 K the intensity of the spectra decreases. The above observations have been reported previously on a 1% Pt/Al_2O_3 catalyst during the heating in CO (58). At room temperature the authors observe a single IR band at 2080 cm^{-1} attributed to the linear CO species adsorbed on platinum atoms. When the temperature is increased, a shift of the IR band is observed (2065 cm^{-1} at 423 K) associated to the detection of a shoulder at 2080 cm^{-1}. This shoulder is attributed to linear CO species adsorbed on platinum atoms existing in small mats or arrays, possibly strongly interacting with the alumina support (58). The authors also observe, without comments, an increase of the intensity of the main IR band during the heating in CO (see Fig. 5 of Ref. (58)). The results of Fig. 10 show that the platinum surface is modified during heating in CO (increase of the intensity of the IR band and detection of the shoulder). The origin of this modification (not observed on the three-way catalyst) is off the scope of the present study, but it can be due, for instance, to a reconstruction of the surface of the platinum particles or to the dissociation of CO, leading to adsorbed carbon and may be adsorbed oxygen.

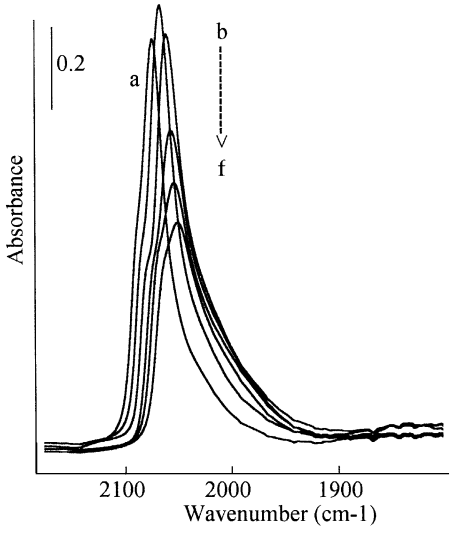

FIG. 10. Infrared spectra taken during the adsorption of CO (1% CO/He) on the Pt/Al_2O_3 catalyst at various temperatures: (a) 378 K; (b) 453 K; (c) 533 K; (d) 633 K; (e) 693 K; (f) 783 K.

Figure 11 indicates the change of the coverage of the sites with the adsorption temperature on Pt/Al_2O_3 (curve a) and $Pt/CeO_2/Al_2O_3$ (curve b). The surface area of the IR band of Fig. 10 (including the shoulder and the main IR band) in the temperature range 480–600 K is used to determine $\theta = 1$. This is justified by the following experiment performed on $Pt/CeO_2/Al_2O_3$ (the same results are obtained on Pt/Al_2O_3): after the adsorption of CO at 373 K on the reduced solid (spectrum a, Fig. 12) (IR band at 2078 cm^{-1}), the temperature is increased to 473 K in 1% CO/He (spectrum b, Fig. 12). At this temperature the shoulder at 2080 cm^{-1} is not detected but it can be considered that the increase of the surface area of the IR band between 373 K and 473 K (ratio [surface area at 373 K/surface area at 473 K] = 0.8) is related to the modification of the surface of the platinum particles which leads to the detection of the shoulder at higher temperatures as observed in Fig. 10 (when the shift of the main IR band permits its detection). The solid is then cooled down to 373 K in CO/He. The spectrum recorded (spectrum c, Fig. 12) is different than

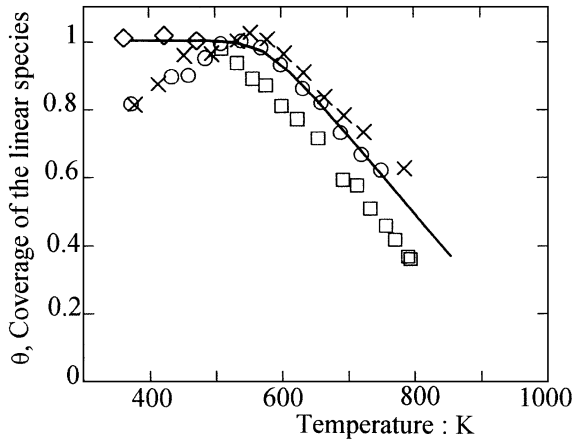

FIG. 11. Evolution of the coverage of the linear CO species with temperature of adsorption: ×, (a) experimental data on Pt/Al_2O_3; ○, (b) experimental data on $Pt/CeO_2/Al_2O_3$; ◇, (c) experimental data on $Pt/CeO_2/Al_2O_3$ during the cooling down from 473 K to 373 K; □, (d) experimental data on $Pt/Rh/CeO_2/Al_2O_3$; ———, (f) coverage according to expression [3] (see the text for the parameters).

the initial spectrum (spectrum a). The intensity is higher and the position of the IR band is 2073 cm^{-1}. The results of Fig. 12 show that the modification of the platinum surface during heating is irreversible. Figure 11, curve c, gives the coverage of the sites during the cooling down from 473 K to 373 K using for $\theta = 1$ the surface area of the IR band at 473 K. It can be observed that the coverage is constant and equal to the values of curve b in the range 480–600 K. This leads to the following comments: (a) modification of the surface of the platinum particles is produced before 480 K; (b) the full coverage of the sites is maintained until around 600 K.

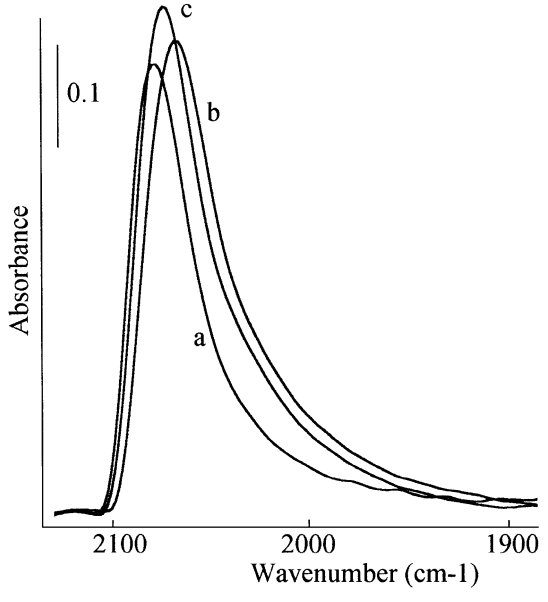

FIG. 12. Infrared spectra taken during the adsorption of CO on $Pt/CeO_2/Al_2O_3$: (a) at 373 K after the pretreatment; (b) at 473 K after the heating from 373 K; (c) at 373 K after cooling from 473 K.

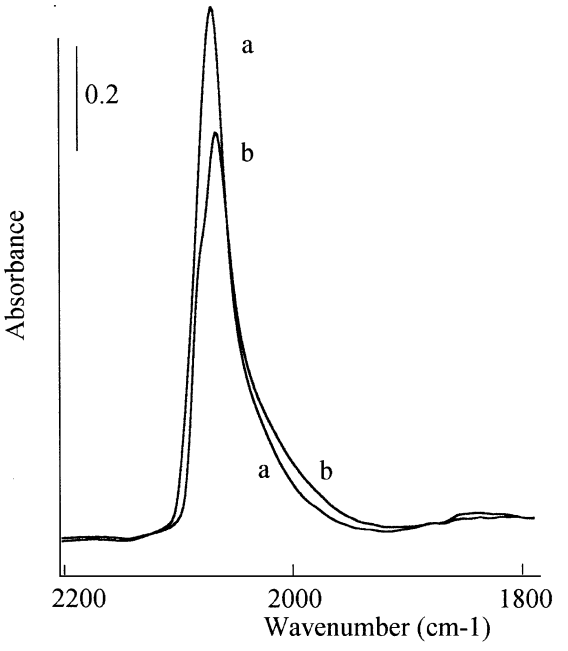

FIG. 13. Infrared spectra taken during the adsorption of CO on Pt/Al_2O_3: (a) at 473 K before the heating at 783 K; (b) at 473 K after cooling from 783 K.

Figure 13 gives the comparison of the FTIR spectra at 473 K on the Pt/Al_2O_3 catalyst before heating in CO/He to 783 K (spectrum a) and after cooling from 783 K to 473 K in CO/He (spectrum b). In this last spectrum some IR bands are detected below 1600 cm^{-1} (not shown), attributed to adsorbed carbonate species due to the CO_2 coming from the disproportionation reaction. As on the three-way catalyst, the deposition of carbon has a limited influence on the IR spectra. However, it can be noted, contrary to the Pt/Rh solid (see Fig. 9), that the two spectra in Fig. 13 are not identical due to the modification of the surface of the platinum particles. This comparison confirms that the bimetallic and the monometallic particles present different evolutions during heating in CO/He.

(f) Heat of Adsorption of CO on the Platinum-Containing Solids

On the two platinum containing solids, the coverage of the sites decreases linearly, after 600 K, with the adsorption temperature (Fig. 11, curves a and b), as observed on the three-way catalyst. To facilitate the comparison, the decreasing section of the curve observed of the three-way catalyst (Fig. 7) is reported on Fig. 11 (curve d). Curves a and b indicate that there are no significant differences between the two platinum-containing solids. The nature of the support, either Al_2O_3 or 20% CeO_2/Al_2O_3, does not strongly

influence the adsorption of CO on the platinum particles. The linearly decreasing profile of the coverage with the adsorption temperature (curves a and b, Fig. 11) permits using the adsorption model described above (expression [3]) to determine the heat of adsorption of CO. The curve e in Fig. 11 is obtained using the following values for the heat of adsorption of CO: $E_1 = 105$ kJ/mol; $E_0 = 195$ kJ/mol. These values are slightly higher: (a) than those found on the three-way catalyst ($E_1 = 97$ kJ/mol; $E_0 = 178$ kJ/mol) and (b) than the values from the literature obtained by microcalorimetric measurements. However, for this last comparison, it must be taken into account the change of the surface of the platinum particles during heating in CO/He recorded in the present study which cannot be observed at the temperatures used during the microcalorimetric measurements. The values of the heat of adsorption found above, on the platinum-containing solids, represent an average of two linear CO species while on the three-way catalyst a single species is concerned and in this case the comparison with the literature seems more valid.

The heats of adsorption of CO on the three solids can be compared at the same coverage, $\theta \approx 0.6$, using expression [1]. The values are 130 kJ/mol on $Pt/Rh/CeO_2/Al_2O_3$, 145 kJ/mol on $Pt/CeO_2/Al_2O_3$, and 150 kJ/mol on Pt/Al_2O_3. The difference of the heat of adsorption of CO between the monometallic solids and the three-way catalyst (around 20 kJ/mol.) is significant (higher than the accuracy of the method) but not very strong. It seems too early to conclude that this difference is only due to the composition of the bimetallic particles. As the experimental method is a very sensitive one the differences observed can be also correlated to other factors such as the modification of the platinum particles on the monometallic solids, the metallic dispersion, or the decoration of the particles. The influence of these parameters on the heat of adsorption of CO must be studied separately.

The present method of determination of the heats of adsorption of the linear CO species at various coverages is experimentally easy. However, the dissociation of CO at high temperature constitutes the weak point. This imposes the use of low partial pressure of CO and the range of temperatures studied (both parameters acting on the coverage). The possible change of the metallic surface during the adsorption at high temperature as observed on the monometallic particle may also constitute an inconvenient. However, it can be noted that an advantage of the present method, compared to microcalorimetric measurements, is that the FTIR spectra allow us to make a distinction between various adsorbed species while microcalorimetric measurements give the average of the various adsorbed species. For instance, it can be possible to measure the heat of adsorption of the bridged CO species, following the decrease of the intensity of the IR band (which must be large enough) with the adsorption temperature.

IV. CONCLUSION

The present paper shows that the heat of adsorption of CO on various platinum containing solids (in particular a three-way catalyst) can be evaluated by the FTIR spectra recorded during the adsorption of CO in the range 300–800 K and using a classical chemisorption model. The values obtained are in agreement with those found in the litterature on platinum containing solids and measured by microcalorimetric methods in particular. The experimental change of the coverage of the main adsorbed CO species with the adsorption temperature is interpreted by a linear variation of the heat of adsorption with the coverage.

ACKNOWLEDGMENT

The authors acknowledge the E.C.I.A Co. (Equipement et Composant pour l'Industrie Automobile), Bavans, France, which supported this work. Thanks are due to Isabelle Blanc for the preparation of the three-way catalyst and to Sylviane Blois for technical assistance during the measurement of the efficiency of the three-way catalyst.

REFERENCES

1. Happel, J., "Isotopic Assessment of Heterogenous Catalysis," Academic Press, New York, 1986.
2. Stockwell, D. M., Bianchi, D., and Bennett, C. O., *J. Catal.* **113**, 13 (1988).
3. Winslow, P., and Bell, A. T., *J. Catal.* **94**, 385 (1985).
4. Bianchi, D., and Gass, J. L., *J. Catal.* **123**, 298 (1990).
5. Balakos, M. W., Chuang, S. S. C., and Sriniavas, G., *J. Catal.* **140**, 281 (1993).
6. Cho, B. K., and Stock, C. J., *J. Catal.* **117**, 202 (1989).
7. Mergler, Y. J., and Nieuwenhuys, B. E., *J. Catal.* **161**, 292 (1996).
8. Krishnamurthy, R., Chuang, S. S. C., and Balakos, M. W., *J. Catal.* **157**, 512 (1995).
9. Nagai, M., Luchietto, l. L., Li, Y. E., and Gonzalez, R. D., *J. Catal.* **101**, 522 (1986).
10. Hicks, R. F., Kellner, C. S., Savatsky, B. J., Hecker, W. C., and Bell, A. T., *J. Catal.* **71**, 216 (1981).
11. Vannice, M. A., Hasselbring, L. C., and Sen, B., *J. Catal.* **97**, 66 (1986).
12. Gorte, R. J., *J. Catal.* **75**, 164 (1982).
13. Demmin, R. A., and Gorte, R. J., *J. Catal.* **90**, 32 (1984).
14. Ioannides, T., and Verykios, X. E., *J. Catal.* **120**, 157 (1989).
15. Sen, B., and Vannice, M. A., *J. Catal.* **130**, 9 (1991).
16. Sharma, S. B., Miller, J. T., and Dumesic, J. A., *J. Catal.* **148**, 198 (1994).
17. Gangal, N. D., Gurta, N. M., and Yier, R. M., *J. Catal.* **140**, 443 (1993).
18. Ahlafi, H., Bennett, C. O., and Bianchi, D., *J. Catal.* **133**, 83 (1992).
19. Bianchi, D., Bouly, C., Gass, J. L., and Maret, D., *Bull. Soc. Chim. Fr.* **128**, 130 (1991).
20. Bianchi, D., Gass, J. L., Bouly, C., and Maret, D., *S.A.E., Paper* **910839** (1992).
21. Little, L. H., "Infrared Spectra of Adsorbed Species," Academic Press, London, 1966.
22. Hair, M. L., "Infrared Spectroscopy in Surface Chemistry," Dekker, New York, 1967.
23. Oltay, E., Penninger, J. M. L., Alemdaroglu, N., and Alberigs, J. M., *Anal. Chem.* **45**, 802 (1973).
24. Peri, J. B., and Hannan, R. B., *J. Phys Chem.* **64**, 1526 (1960).
25. Bianchi, D., Lacroix, M., Pajonk, G., and Teichner, S. J., *J. Catal.* **59**, 467 (1979).

26. Little, L. H., Kluser, H. E., and Amberg, C. H., *Can. J. Chem.* **39**, 42 (1961).
27. Kokes, R. J., Dent, A. L., Chang, C. C., and Dixon, L. T., *J. Amer. Chem.* **94**, 4429 (1972).
28. Ueno, A., Hochmuth, J. K., and Bennet, C. O., *J. Catal.* **49**, 225 (1977).
29. Moon, S. H., Windawi, H., and Katzer., *Ind. Eng. Chem. Fund.* **20**, 396 (1981).
30. Jackson, S. D., Glanville, B. M., Willis, J., McLellan, G. D., Webb, G., Moyes, R. B., Simpson, S., Wells, P. B., and Whyman, R., *J. Catal.* **139**, 207 (1993).
31. Bianchi, D., and Teichner, S. J., *Bull. Soc. Chim. Fr.* **7**, 1463 (1975).
32. Penninger, J. M. L., *J. Catal.* **56**, 287 (1979).
33. Yokomizo, G. H., Louis, C., and Bell, A. T., *J. Catal.* **120**, 1 (1989).
34. Fisher, I. A., and Bell, A. T., *J. Catal.* **172**, 222 (1997).
35. Robbins, J. L., *J. Catal.* **115**, 120 (1989).
36. Zhou, X., and Gulari, E., *Langmuir* **4**, 1332 (1988).
37. Chuang, S. S. C., and Pien, S. I., *J. Catal.* **135**, 618 (1992).
38. Chuang, S. S. C., Srinivas, G., and Mukherjee, A., *J. Catal.* **139**, 490 (1993).
39. Chuang, S. S. C., Brundage, M. A., Balakos, M. W., and Srinivas, G., *Appl. Spectrosc.* **49**, 1151 (1995).
40. Batis, H., Bianchi, D., Bennett, C. O., Pajonk, G., and Teichner, S. J., "Proc. IV ICSS-III ECOSS 1980," Vol. 1, p. 529.
41. Chafik, T., *thesis*, Lyon, 1993.
42. Savargaonkar, N., Khanra, B. C., Pruski, M., and King, T. S., *J. Catal.* **162**, 277 (1996).
43. Cai, Y., Stenger, H. G., Jr., and Lyman, C. E., *J. Catal.* **161**, 123 (1996).
44. Lakis, R. E., Lyman, C. E., and Stenger, H. G., Jr., *J. Catal.* **154**, 261 (1995).
45. Armor, J. N., *Appl. Catal., B. Environ.* **1**, 221 (1992).
46. Engler, B. H., Lindner, D., Lox, E. S., Schafer-Sindilinger, A., and Ostgathe, K., *Stud. Surf. Sci. Catal.* **96**, 441 (1995).
47. Anderson, J. A., *J. Catal.* **142**, 152 (1993).
48. Van Slooten, R. F., and Nieuwenhuys, B. E., *J. Catal.* **122**, 429 (1990).
49. Primet, M., Basset, J. M., Mathieu, M. V., and Prettre, M., *J. Catal.* **29**, 213 (1975).
50. Barth, R., Pitchai, R., Andreson, R. L., and Verykios, X. E., *J. Catal.* **116**, 61 (1989).
51. Vaarkamp, M., Miller, J. T., Modica, F. S., and Koningsberger, D. C., *J. Catal.* **163**, 294 (1996).
52. Mergler, Y. J., van Aalst, A., van Delft, J., and Nieuwenhuys, B. E., *J. Catal.* **161**, 310 (1996).
53. Efstahiou, A. M., Chafik, T., Bianchi, D., and Bennett, C. O., *J. Catal.* **147**, 24 (1994).
54. Angevaare, P. A. J. M., Hendrickx, H. A. C. M., and Ponec, V., *J. Catal* **110**, 18 (1988).
55. Srinivas, G., and Chuang, S. S. C., *J. Catal.* **144**, 131 (1993).
56. Efstathiou, A. M., Chafik, T., Bianchi, D., and Bennett, C. O., *J. Catal.* **148**, 224 (1994).
57. Buchanan, D. A., Hernandez, M. E., Solymosi, F., and White, J. M., *J. Catal.* **125**, 456 (1990).
58. Anderson, J. A., and Rochester, C. H., *J. Chem. Soc. Faraday Trans.* **87**, 1479 (1991).
59. Rasband, P. B., and Hecker, W. C., *J. Catal.* **139**, 551 (1993).
60. Clark, A., "The Theory of Adsorption and Catalysis," Academic Press, London, 1970.
61. Tompkins, F. C., "Chemisorption of Gases on Metal," Academic Press, London, 1978.
62. Solymosi, F., and Pasztor, M., *J. Catal.* **104**, 312 (1987).